

NUMERICAL ANALYSIS OF CONDUCTOR RESPONSE TO FAST-RISING HIGH-CURRENT PULSES

Center for Electromechanics
The University of Texas at Austin
Balcones Research Center
Building 133
Austin, TX 78758-4497

R. W. Cook and J. L. Bacon

A computer code has been developed to rapidly evaluate the response of a collection of conductors of arbitrary geometry to a fast-rising, high-current pulsed discharge. The code applies to any set of conductors which are long compared to their transverse dimensions (2-D limit). The high frequency diffusion limited current distribution is evaluated to determine the high frequency inductance and resistance, the surface temperature rise and the local magnetic stress and total force on each conductor for a specified peak current. The model has been validated against analytic solutions for simple geometries and experimental results for more intricate geometries. The code is optimized for fast computation, facilitating an iterative design procedure for arbitrary conductor assemblies.

The design of conductors employed in fast-rising, high current pulsed power applications requires accurate evaluation of their inductances, resistances, and mechanical support requirements. Current distributions must be determined to compute localized heating, local pressures, and net forces between conductors. Hand calculation of these effects is possible only in simple approximations while finite element methods generally require substantial mainframe computation time as well as considerable overhead in "setting up" different case geometries. A computer code which falls between these extremes has been developed to analyze these effects for systems of conductors of arbitrary geometry. The model proves to be very accurate for conductors that are long compared to their cross-sectional dimensions and for discharge times short enough that the magnetic diffusion depth into the conductors is small compared to their cross-sectional dimensions.

Mathematical Formulation

The starting point of the modeling effort was with the basic formulation of Leuer[1] which is well suited to determining the inductance gradient and current distribution on a collection of arbitrarily shaped long parallel conductors in the high frequency limit. A brief description of the formulation is given here. Maxwell's steady state equations for regions of constant permeability result in Poisson's equation for the magnetic vector potential, A , with the current density, j , as the source term. In the high frequency limit, all conductor currents flow in thin sheets on the conductor surfaces (skin depth), and the magnetic field inside the conductors is zero. The magnetic vector potential throughout each conductor must therefore be constant, and the problem is reduced to solving Laplace's equation between the conductors with the constant values of the magnetic vector potential on the conductors as the boundary values. If the conductors are taken to be infinitely long (long compared to their transverse dimensions) carrying parallel currents, then the magnetic vector potential is one-dimensional and directed parallel to the conductor currents.

By assuming the surface currents in each conductor can be approximated as a collection of infinitely long current sheets, each carrying a uniform sheet current density, K , the problem can be reduced to matrix form. An analytic expression for the magnetic vector potential contribution of each current sheet is used, and the sum of these contributions over all current sheets is constrained to produce the constant boundary values of magnetic vector potential at selected points on the conducting surfaces. The use of a collection of current sheets to depict the conductor currents avoids the singularities that occur in filamentary models. This describes the essential features of the basic formulation, although the details of implementation in this work differ slightly from that of Leuer.

The magnetic vector potential generated at any point (x, y) by a vanishingly thin current sheet located at $x = 0$ and extending from $y = -h$ to $y = +h$ can be solved analytically and expressed as:

$$\begin{aligned} A(x, y) = -\mu_0 K / 2\pi & \{ x [\tan^{-1}((y + h)/x) \\ & - \tan^{-1}((y - h)/x)] \\ & + (y + h) \ln([(y + h)^2 + x^2]^{\frac{1}{2}}) \\ & - (y - h) \ln([(y - h)^2 + x^2]^{\frac{1}{2}}) \} \quad (1) \end{aligned}$$

We assume throughout this work that the sheet is infinite in the z direction with its current in the positive or negative z direction. The potential at any point in the $x-y$ plane due to a current sheet arbitrarily positioned in the plane can then be determined by computing the point's coordinates in the frame of reference of the current sheet as described above and evaluating equation (1).

The potential at any point (x_i, y_i) due to a collection of N current sheets can be expressed:

$$A(x_i, y_i) = \sum_{j=1}^N K_j a_j(x_i, x_j, y_i, y_j) \quad (2)$$

where $a_j = A_j/K_j$, depending on position only. If the N current sheets describe M conductors, there are then N unknown current sheet densities and M unknown values of constant magnetic vector potential. By choosing N points, (x_i, y_i) , at which to evaluate the potential using equation (2), N equations are generated. By constraining the sum of current over all the sheets on a particular conductor to be a specified current or:

$$I = \sum_j K_j l_j \quad (3)$$

where

l_j = width of the j th sheet

| Report Documentation Page | | | Form Approved OMB No. 0704-0188 | |
|---------------------------------------------------------------------------------------------------------------------------------------------------------------------------------------------------------------------------------------------------------------------------------------------------------------------------------------------------------------------------------------------------------------------------------------------------------------------------------------------------------------------------------------------------------------------------------------------------------------------------------------------------------------------------------------------------------------------------------------------------------------------------------------------------------------------------------------------------------------|------------------------------|------------------------------|-------------------------------------------------|----------------------------------------|
| <p>Public reporting burden for the collection of information is estimated to average 1 hour per response, including the time for reviewing instructions, searching existing data sources, gathering and maintaining the data needed, and completing and reviewing the collection of information. Send comments regarding this burden estimate or any other aspect of this collection of information, including suggestions for reducing this burden, to Washington Headquarters Services, Directorate for Information Operations and Reports, 1215 Jefferson Davis Highway, Suite 1204, Arlington VA 22202-4302. Respondents should be aware that notwithstanding any other provision of law, no person shall be subject to a penalty for failing to comply with a collection of information if it does not display a currently valid OMB control number.</p> | | | | |
| 1. REPORT DATE JUN 1989 | 2. REPORT TYPE N/A | 3. DATES COVERED - | | |
| 4. TITLE AND SUBTITLE Numerical Analysis Of Conductor Response To Fast-Rising High-Current Pulses | | | 5a. CONTRACT NUMBER | |
| | | | 5b. GRANT NUMBER | |
| | | | 5c. PROGRAM ELEMENT NUMBER | |
| 6. AUTHOR(S) | | | 5d. PROJECT NUMBER | |
| | | | 5e. TASK NUMBER | |
| | | | 5f. WORK UNIT NUMBER | |
| 7. PERFORMING ORGANIZATION NAME(S) AND ADDRESS(ES) Center for Electromechanics The University of Texas at Austin Balcones Research Center Building 133 Austin, TX 78758-4497 | | | 8. PERFORMING ORGANIZATION REPORT NUMBER | |
| 9. SPONSORING/MONITORING AGENCY NAME(S) AND ADDRESS(ES) | | | 10. SPONSOR/MONITOR'S ACRONYM(S) | |
| | | | 11. SPONSOR/MONITOR'S REPORT NUMBER(S) | |
| 12. DISTRIBUTION/AVAILABILITY STATEMENT Approved for public release, distribution unlimited | | | | |
| 13. SUPPLEMENTARY NOTES See also ADM002371. 2013 IEEE Pulsed Power Conference, Digest of Technical Papers 1976-2013, and Abstracts of the 2013 IEEE International Conference on Plasma Science. Held in San Francisco, CA on 16-21 June 2013. U.S. Government or Federal Purpose Rights License. | | | | |
| 14. ABSTRACT | | | | |
| 15. SUBJECT TERMS | | | | |
| 16. SECURITY CLASSIFICATION OF: a. REPORT unclassified | | | 17. LIMITATION OF ABSTRACT SAR | 18. NUMBER OF PAGES 7 |
| b. ABSTRACT unclassified | | | | |
| c. THIS PAGE unclassified | | | | |

then M equations are generated, and the problem is completely specified. The system of equations can be written in matrix form and inverted to solve for the unknowns. The advantages of this formulation over one which arbitrarily specifies the potentials on each conductor are that the actual values of the potential are determined, and that the specification of total current in each conductor is a much more natural and intuitive task. The disadvantage is that the system of equations loses its symmetry. It can be shown that the system of N equations generated by applying equation (1) to N points can yield a Toeplitz matrix which can be inverted much more quickly than a non-symmetric matrix[2]. For highly complex systems, the ease of inversion might be important.

In this formulation, the N points chosen to apply equation (2) were taken to be the midpoints of the N current sheets.

Once the surface current distribution and magnetic vector potential constants are known, the inductance can be computed from energy considerations. The gradient of the stored magnetic energy can be expressed:

$$d/dz(E_M) = \iint (j \cdot A) dx dy = \sum_{j=1}^N (K_j/l_j) A_j \quad (4)$$

where here A_j denotes the magnetic vector potential constant on the j'th current sheet. This can be equated to an inductive energy gradient of:

$$d/dz(E_M) = L' I^2 / 2 \quad (5)$$

where L' is the inductance gradient and I is the total current, so that:

$$L' = (2/I^2) \sum_{j=1}^N A_j K_j / l_j \quad (6)$$

The magnetic pressure on any current sheet surface element follows immediately from the relations:

$$B = \mu_0 K \quad (7)$$

$$p = B^2 / 2\mu_0 \quad (8)$$

Equation (7) holds for the field immediately outside a conductor having a surface current density, K , and zero field inside the conductor. The B field is found to be parallel to the surface element, and the magnetic pressure indicated by (8) acts perpendicular into the surface element.

The total force per unit length on a conductor is easily computed by integrating the magnetic pressure on the current sheet surface elements over all the elements on that conductor, or:

$$d/dz(F) = - p n dl = \sum_j^{\text{conductor}} -(\mu_0 K_j)^2 / 2 n \quad (9)$$

where dl integrates over the conductor circumference and n is the surface normal.

The evaluation of resistance and ohmic temperature rise on conductors carrying fast-rising high-currents requires an evaluation of the nonlinear current diffusion into the conductors. For skin

depths small compared to the conductor dimensions, this diffusion may be considered one dimensionally inward from the conductor surface. The problem of 1-D diffusion of current into a conductor and the ohmic heating of that conductor was analyzed by Kidder[3] or a step function magnetic field applied at $t = 0$ (i.e., step function current waveform). The processes were found to depend only upon the variable x/δ where $\delta = \beta t^{1/2}$ is a characteristic "skin depth" and β is a constant which depends upon the properties of the conducting material.

A computer code based on Kidder's formulation was developed to determine detailed response of different conducting materials to 1-D diffusion. The solutions obtained differed from Kidder's in that the temperature dependence of the conductivity was considered as well as the thermal conductivity of the material (assumed constant). In one dimension the problem reduces to ordinary nonlinear differential equations subject to boundary values. The equations were solved using a predictor-corrector integrator routine which was iterated, starting with initial guesses for the unknown initial conditions (magnetic field gradient, and surface temperature rise on the conducting surface), to find the correct initial conditions to satisfy the boundary values (zero field and temperature rise far into the conductor). This process was repeated for various field strengths and was completed for copper, aluminum, and molybdenum. The initial conditions thus determined are shown for copper as a function of the initial current density (field) in figure 1. By fitting a curve to the first plot, the surface temperature rise for copper at a given surface current density can be computed to be approximately:

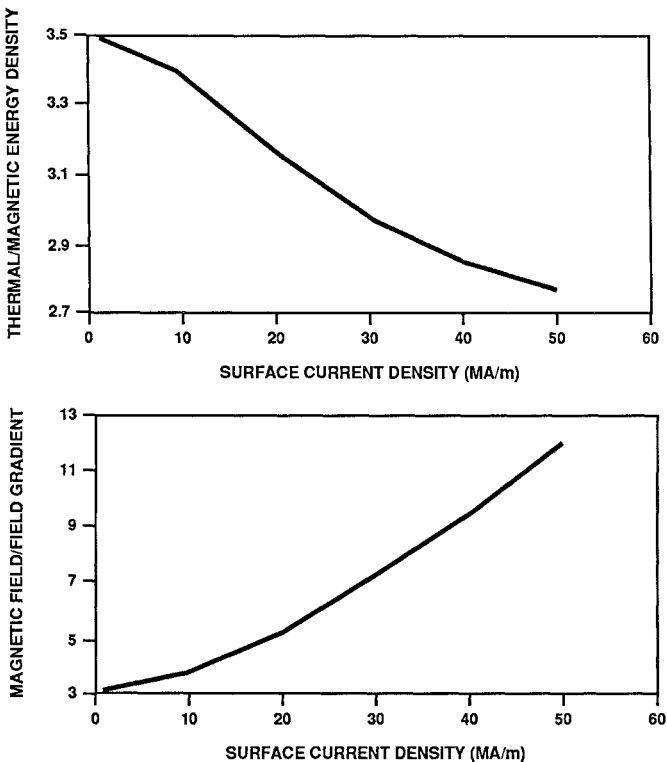


Figure 1. One-dimensional current diffusion, relation of boundary to initial conditions

$$\rho C_p \Delta T = \mu_0 K^2 / 2 [2.7 + 0.8 \exp(-0.141 K^2 / 10^7)] \quad (10)$$

Similar curves were derived for the other metals.

In the 1-D limit, assuming a step current rise, the conductor surface temperature is found to rise instantaneously with the initiation of current to the peak value given by equation (10). The temperature rise on the interior of the conductor is time dependent with fixed isotherms propagating into the conductor as $t^{1/2}$. Plots of the interior temperature rise as a function of the number of skin depths are shown in figures 2 and 3 for copper at surface current densities of 30 MA/m and 50 MA/m. From the 50 MA/m case it is clear that with a 10% increase in current density over the critical current density of 45 MA/m, melting will be observed over a full 1/3 of a skin depth. The critical currents for copper, aluminum and molybdenum were determined from this analysis to be 45, 28 and 56 MA/m respectively. This agrees well with a closed form analysis presented by Knoepfle[4] which yields corresponding values of 42, 30, and 61 MA/m disregarding the temperature dependence of the resistivity.

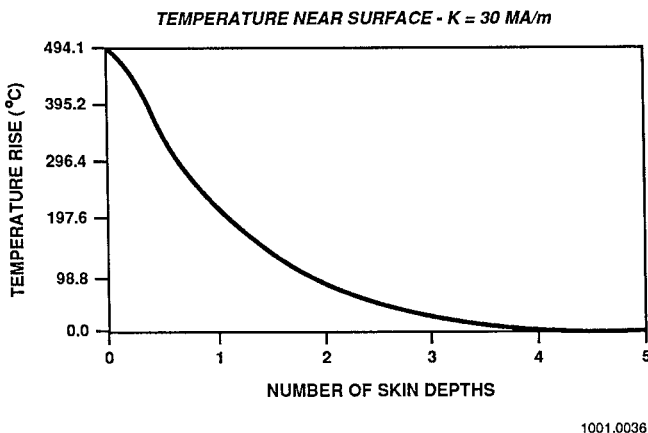


Figure 2. Conductor surface temperature rise as a function of the number of skin depths into the material for room temperature copper with current density of 30 MA/m

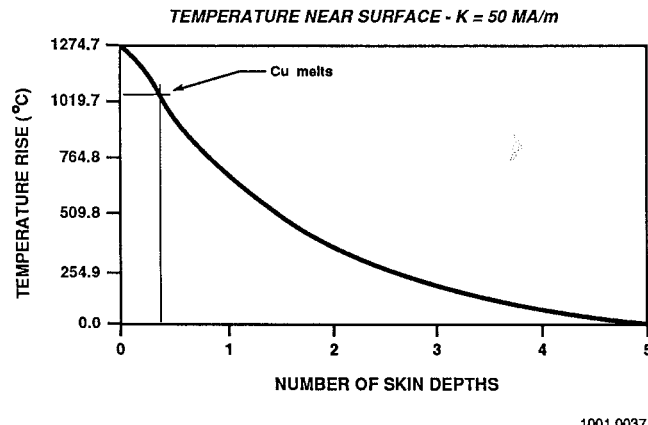


Figure 3. Conductor surface temperature rise as a function of the number of skin depths into the material for room temperature copper with current density of 50 MA/m

Knoepfle shows that current waveforms with slower rise times change the critical current density only by a maximum factor of about 1.7. The critical current density may be considered a fundamental limit to conductor capability.

To model the time dependent resistance, the 1-D diffusion of current in a surface current sheet was integrated to determine a j^2 power loss. The total power loss over all the sheets was then summed, and that loss was equated to an I^2R resistive power loss, resulting in the expression:

$$R' = \rho [\mu_0 / (2\pi t\rho)]^{1/2} \sum_{j=1}^N (f_j)^2 / l_j \quad (11)$$

where

ρ = room temperature resistivity of the material

t = time since current started

f_j = fraction of total current carried by j th sheet

R' = resistance per unit length of the conductor

Equation (11) was derived ignoring the increase in resistivity with temperature. Including the temperature rise information increases the total resistance by 30% for critical current densities, and less so for lower current densities. If the current density is lower than the critical current density or non-uniform, the resistance determination accuracy from equation (11) will improve.

Program Implementation

The coding of the model formulated above was done in Pascal under the program name of LPRIME. Versions of LPRIME were developed for the IBM PC, the Apple Macintosh and the Vax 11-750 computers. Initially the code was designed to be used interactively, although in some applications the input and output have been taken from and directed to disk files.

The code will allow up to 20 conductors to be arbitrarily positioned in a 2-D cross section with arbitrary currents. The user describes the cross-section of each conductor as a set of up to 20 linear, circular, or elliptic curves. During this input procedure, a graphical display of the specified curves can be generated to verify the accuracy of the input data. The total current for each conductor is also specified by the user, although the magnitude of current does not affect the inductance gradient determination. In order to correctly evaluate the total force it is necessary that the conductor curves be described in sequence as one would "walk" around the perimeter of the conductor in a clockwise direction.

The system of conductors described is automatically broken down into an approximately equivalent set of current sheet elements distributed evenly between the conductors in the system and evenly around the surface of the conductor. The maximum total number of elements is limited on personal computers by available memory to several hundred, and on the Vax by excessive runtimes to about one thousand. This gives a practical limit to the complexity of the systems which can successfully be modeled.

Once the conductors have been broken into elements, the program assembles and solves the matrix of equations which determines the surface current density and vector potential for each element. A 300 element double-precision run requires about half an hour on an IBM-XT with a coprocessor and about three minutes on the Vax. Although no detailed analysis has been completed on the question of round-off errors in this application, it was noticed that at a 300 element matrix size, the results of single and double precision runs were beginning to differ. Therefore the maximum number of elements that can be used may also be limited by round-off error. In order to run a 300 element case in double precision on the PC the matrix was simultaneously loaded and solved, with the lower half of the matrix "folded" up into the blank memory left as the matrix was diagonalized. Otherwise, the matrix solver was a straight-forward Gaussian elimination method.

As output, LPRIME reports the inductance gradient, a resistive coefficient equivalent to $C_R = R't^{1/2}$ (see equation (11) above), and the components of the net force on each conductor. Graphs of the current density, surface temperature rise and normal magnetic pressure over the conductor perimeter are displayed to the screen for all conductors in the system. An example of the graphical output is shown in figure 4 for a circular bore railgun (see Task B geometry described in validation section for details).

Before terminating, the program allows the user to loop back to the input to change any or all of the input parameters, facilitating the parametric analysis of various conductor configurations.

In exercising the code it was discovered that the model starts to break down when the distance between adjacent conductors becomes comparable to the size of the current sheet elements. The element size also gives an effective corner radius when attempting to model rectangular conductors.

The program was formulated with the implicit assumption that all conductors carrying current in a particular direction operated in parallel. If those conductors are connected in series, however, the current distributions, temperature rises, and magnetic pressures predicted by the code are still valid, and the inductance gradient value can be corrected by a factor of N^2 where N is the number of series connected conductors. For some augmented railguns where a series turn extends the entire length of the bore, the inductance gradient must be further corrected to account for the different regions ahead and behind the projectile to arrive at the correct driving inductance gradient.

Validation of the Numerical Results

The results of the code have been validated against known analytic solutions, detailed finite element simulations and experimentally measured values. Generally the agreement is excellent in comparing analytic solutions for simple cases and experimental values. Less agreement is found in more complex cases where the analytic solution or finite element analysis employs simplifying assumptions, although the agreement is still good.

The code results for inductance gradient (I_{prime}) and magnetic force per unit length (f_{prime}) were compared to known values for six different geometries. These included parallel filaments, coaxial conductors, parallel current sheets, parallel plates, four fila-

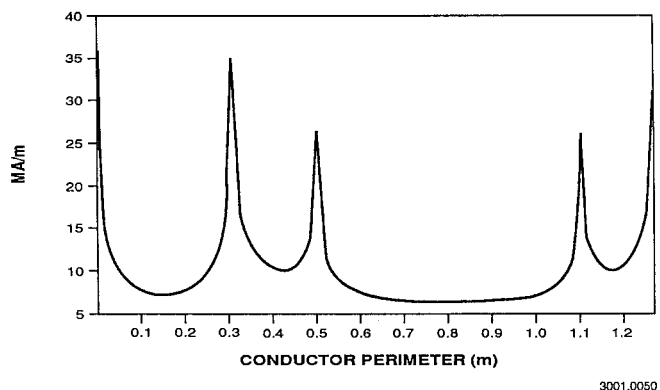


Figure 4a. Current density

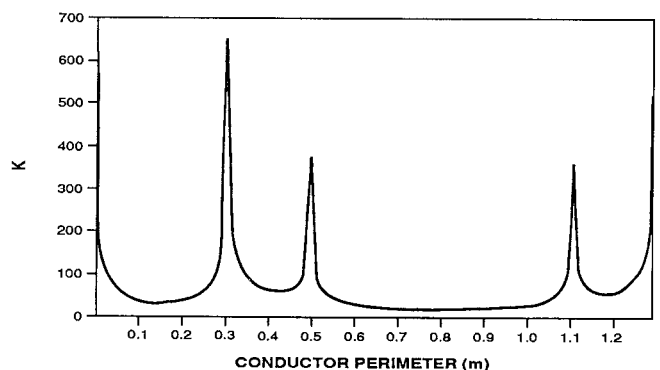


Figure 4b. Surface temperature rise

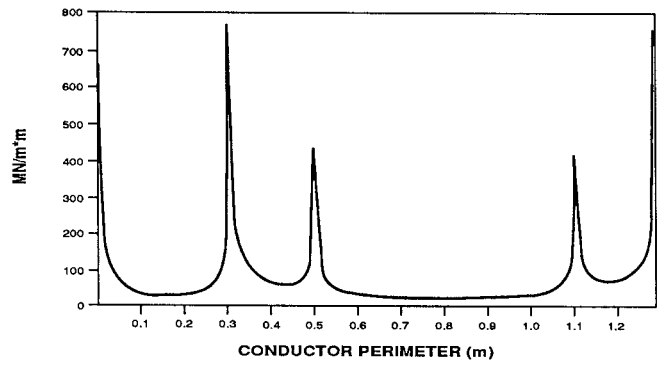


Figure 4c. Magnetic loading on surface

Figure 4. Sample output from LPRIME code for Task B geometry

ments in a rectangular orientation and a geometry used in a railgun built at CEM-UT (Task B geometry).

The parallel filament geometry consisted of two conductors having 1 mm diameters separated by 2 cm and carrying equal and opposite currents equal to 5 kA. Values of 1.4754 $\mu\text{H}/\text{m}$ and 250.29 N/m were predicted for the inductance gradient and the force gradient respectively. The closed form solution for parallel filaments yields the values of 1.4655 $\mu\text{H}/\text{m}$ and 250.00 N/m.

The coaxial geometry assumed an inner conductor radius of 2 cm and an outer conductor radius of 4 cm. The conductors carried equal and opposite currents of 5 kA. Inductance and force gradients were 0.1386 $\mu\text{H}/\text{m}$ and 0.0 N/m respectively, agreeing exactly with the closed form solutions.

The next two geometry cases, parallel current sheets and parallel plates differed only in their thicknesses. Both the current sheets and the plates were 10 cm wide and were separated by a distance of 2 cm, but the plates had a thickness of 1 cm while the sheets were given a smaller thickness of 0.1 cm in order to simulate an infinitely thin conductor. Both the current sheets and the plates were simulated at 5 kA current. The current density plots for the parallel current sheet showed the majority of current flowing uniformly on the inner faces of the conductors with spikes at the ends about triple the magnitude of the value along the inner faces. The predicted value for the inductance gradient of the current sheets was 0.1916 $\mu\text{H}/\text{m}$. A uniform current model which does not consider the end effects nor the existence of a rear surface yields 0.2513 $\mu\text{H}/\text{m}$. The force gradient was predicted to be 96.29 N/m while a formula derived by Dwight[5] gives 105.0 N/m.

For the parallel plates, the predicted value of inductance gradient was 0.1834 $\mu\text{H}/\text{m}$ which agrees exactly with the value calculated using an equation developed by Kerrisk[6]. The force gradient prediction of 89.53 N/m compares to the value of 95.11 N/m from Dwight's formula.

The next geometry case consisted of four filament conductors placed in a rectangular orientation. The spacing of the filaments was based on the Task B railgun geometry - as if the filaments were located at the front edges of the rails. Each filament carried a current of 1.5 MA. The top two conductors carried currents in the opposite direction with respect to the bottom conductors. Predicted values were 1.3581 $\mu\text{H}/\text{m}$ for the inductance gradient and 21.47 MN/m for the force gradient. A code developed at CEM-UT by Albert Wu for predicting axial forces on solenoids predicted a force gradient of 21.9 MN/m[7].

The Task B geometry was analyzed using a current of 3.0 MA, and the analysis was completed both with and without an outer conducting shell which represents the outer containment structure. The inductance gradient was predicted at 0.3661 $\mu\text{H}/\text{m}$ with the outer shell and 0.4224 $\mu\text{H}/\text{m}$ without the outer shell. The experimentally measured value for the inductance gradient was 0.367 $\mu\text{H}/\text{m}$. The total force on the rails per unit length was predicted to be 7.81 MN/m with the outer shell and 13.11 MN/m without it. An experimentally measured value for the force has not been obtained. If the filament formula is applied to two conductors spaced 88.9 mm apart carrying equal and opposite currents with a magnitude of 3.0 MA the repulsion force would be 20.33 MN/m. This method of calculating repulsion force takes no account of the current which is conducted on the edge sides and the

back side of the conductor, nor does it account for the presence of an outer conducting shell. Also it overlooks the current concentration on the rail corners.

The results of the geometry comparisons are summarized in figure 5. The predicted values agree within one percent with the closed form solution values for the parallel filaments and coaxial conductors. In the case of parallel current sheets the predicted value for the force gradient is within 10 percent of the calculated value using Dwight's equations which assume a constant current density distribution over the sheet. The predicted inductance gradient for parallel plates agrees to four significant figures with the value calculated using Kerrisk's equation, and the force gradient agrees with Dwight's equation to within 7 percent. The force gradient prediction for the four filament geometry agrees within 2 percent with Wu's independent computer coding of the same problem. The inductance gradient predicted for the Task B railgun is within one percent of the experimentally measured value.

| GEOMETRY |  |  |  |  |  |  |
|---------------------------------------------------------|-----------------------------------------------------------------------------------|-------------------------------------------------------------------------------------|-------------------------------------------------------------------------------------|-------------------------------------------------------------------------------------|-------------------------------------------------------------------------------------|-------------------------------------------------------------------------------------|
| Current (kA) | 5 | 5 | 5 | 5 | 1.5 E3 | 3.0 E3 |
| I Prime ($\mu\text{H}/\text{m}$) | 1.4754 | 0.1386 | 0.1916 | 0.1834 | 1.3581 | 0.4224 0.3661* |
| I Prime ($\mu\text{H}/\text{m}$) (comparison case) | 1.4655(1) | 0.1386(2) | --- | 0.1834(3) | --- | 0.367(6) |
| F Prime (N/m) | 250.29 | 0.00 | 96.29 | 89.53 | 21.47 E6 | 13.11 E6 7.81 E6* |
| F Prime (N/m) (comparison case) | 250.00(1) | 0.00(2) | 105.00(4) | 95.11(4) | 21.9 E6(5) | 20.33(1) |

(1) Filament Formula (4) H. B. Dwight
 (2) Coax Formula (5) Albert Wu
 (3) J. F. Kerrisk (6) Experimentally measured

* With outer sleeve

3001.0053

Figure 5. Summary of LPRIME code validation work

The validity of the current distribution determination from this formulation was verified by Leuer [1] for the case of parallel conducting cylinders. Additionally the coaxial case shows a constant current distribution on the surface of both inner and outer conductors as would be expected. No other detailed numerical evaluations of the current distribution curve predictions have yet made.

The validity of the temperature rise model was discussed in the description of the formulation. Additionally, the temperature rise predictions for various geometries have been compared to a detailed two-dimensional transient finite element railgun model developed by Long [8]. The finite element model predicts lower temperature rises by about twenty percent, most likely due to the more correct modeling of finite current risetimes (whereas the LPRIME code is based on a step current with an instantaneous rise). Still the agreement is adequate for some design work, and LPRIME is much quicker than the finite element model which require about an hour to run on the Cray XMP 24.

The numerical accuracy of the resistance model has not been examined in detail, as the transient resistance of the systems analyzed thus far at CEM-UT has been much less critical in the design work than the other computed values. Initial checks of the

results have shown the values to be in rough agreement with approximations which assume a constant current density over the conducting surfaces.

Practical Applications

The program was initially developed for use in analyzing the detailed response of various railgun geometries to the high current pulses required during the acceleration. One strong motivation was to develop the capability to rapidly evaluate non-symmetric geometries. Once the code had been completed, it was found to be well suited to the analysis of high-current buswork as well. In addition the code has proved invaluable as a starting point from which to effect more detailed calculations of conductor phenomena. Specifically, the results of the code have been used to provide initial conditions for a temperature relaxation model developed to evaluate cooling requirements for rapid-fire railguns, and as boundary values for finite element structural evaluations of various conductors.

In a railgun design analysis, the LPRIME code was used to determine the force and inductance gradients for two-rail, four-rail and six-rail configurations (shown in figure 6). All of the configurations had bore diameters of 88.9 mm and the arc widths for the rails and insulators were equal. This resulted in arc widths of 90, 45 and 30 degrees for the respective cases. None of the configurations included an outer conducting shell. The computed values are shown for both parallel and series connection of the rail pairs, where a rail pair refers to the two rails which provide the current feed and return for a particular armature. For example, if the four rail configuration is connected in parallel, two current feeds and two current return paths would have to be provided to the gun, while if the rail pairs are connected in series only one current feed and one current return path would be needed.

| GEOMETRY | Parallel Connection | | | Series Connection | | |
|-----------------------|---------------------|--------|--------|-------------------|--------|--------|
| | | | | | | |
| Current Per Rail (MA) | 3 | 1.5 | 1 | 3 | 1.5 | 1 |
| L Prime (μ H/m) | 0.4224 | 0.1498 | 0.0798 | 0.4224 | 0.5992 | 0.7182 |
| F Prime (MN/m) | 13.11 | 3.03 | 1.19 | 13.11 | 3.03 | 1.19 |

3001.0054

Figure 6. Railgun design analysis completed using LPRIME code

The repulsion force per unit length is the same for both methods of rail connection since the magnetic fields depend only on the rail geometries and the total current provided to the gun. If the rail pairs are connected in parallel the inductance gradient drops by a factor of 2.8 when the number of rails is increased from 2 to 4, and by 1.9 when the number of rails is increased from 4 to 6. However, when the rail pairs are connected in series the inductance gradient increases by factors of 1.4 and 1.2 as the number of rails is increased from 2 to 4 and then from 4 to 6. Series connection of the rail pairs does have

the drawback of higher resistance, and it requires a higher driving voltage to produce the desired current.

The LPRIME code was used to verify the inductance of an extremely low inductance buswork designed for use with the CEM-UT 60 MJ homopolar generator power supply. Also the code was used to evaluate the non-uniform current distribution in buswork at the breech of a railgun. The buswork was failing at high currents, and the LPRIME code was used to verify that excessive currents densities were actually occurring and to redesign the buswork to moderate the extremes of the current distribution.

The code output can also be used in structural analysis. The magnetic pressure data is written to an output file for the intended use as boundary loading input for a structural finite element analysis (SFEA). The data for each current sheet element is written to a file. This file contains the midpoint coordinates and the magnetic pressure for each element.

The magnetic pressure can be input into a SFEA in two ways. In the first and least desirable method, the magnetic pressure can be translated into nodal forces and applied individually to each node. This requires for every element present on the surface of the SFEA model, that the magnetic pressure present on the geometrically corresponding location on the LPRIME conductor be multiplied by the element's surface area to obtain a nodal force. Although laborious in nature, this procedure provides a very accurate loading profile. In the second method, through the use of PATRAN (a 3-D MCAE software system) the pressure profile can be approximated by a cubic line by one of several software options that PATRAN offers. PATRAN then performs the translation from the pressure profile to nodal forces and prepares the loading input for several of the major SFEA codes. While this method offers the greater ease, care must be taken that the pressure profile is approximated with the desired accuracy. Irregular profiles may require the first method of loading input.

In addition to the structural finite element analysis, thermal finite element analysis has been completed using the surface temperatures predicted in the LPRIME code as the boundary conditions. The coordinates and temperature of all the surface elements were written to a file and the temperature at associated nodal locations was interpolated from the data. In the analysis done at CEM, another 2-D filament model was used to generate temperature data for the conductor interior. The subsequent evolution of the temperature profile was then simulated for different rail cooling schemes and for various gun geometries.

CONCLUSIONS

Accurate numerical modeling of the transient response of conductors to fast-rising high-current pulses has been accomplished with a computer code which is able to simulate arbitrary geometries of parallel multi-conductor systems and is suitable for use on personal as well as mainframe computers. The code determines non-uniform current distributions in the high frequency limit, diffusion limited ohmic heating and both local and total magnetic forces on the individual conductors as well as evaluating the inductance and resistance of the system of conductors. The model has been validated against various theoretical models and experimental results to establish its accuracy. The code has been successfully applied to the problem of railgun and buswork design, and has been used in conjunction with finite element methods

to analyze temperature relaxation in conductors and evaluate mechanical stresses in conductors with a complex geometry. Although there are practical limits to the complexity of the systems that can be successfully modeled, it is a versatile tool for analyzing a wide range of conductor configurations.

ACKNOWLEDGMENT

We wish to thank Kurt Nalty, Mike Ingram and Joe Beno for their helpful conversations and suggestions during the development and testing of this program. The code was developed under funding provided by the Air Force Armament Testing Laboratory.

REFERENCES

1. J. A. Leuer, "Electromagnetic Modeling of Complex Railgun Geometries," IEEE Transactions on Magnetics, Vol. MAG-22, No. 6, November 1986, pp. 1584-1590.
2. W. H. Press, B. P. Flannery, S.A. Teukolsky and W. T. Vetterling, Numerical Recipes, Cambridge University Press, Cambridge, 1986.
3. R. E. Kidder, "Nonlinear Diffusion of Strong Magnetic Fields into a Conducting Half-Space," UCRL-5467, TID-4500 (14th edition).
4. H. Knoepfel, Pulsed High Magnetic Fields, American Elseview Publishing Company, Inc., New York, 1970.
5. H. B. Dwight, "Repulsion Between Strap Conductors," Electrical World, Vol. 70, No. 11.
6. J. F. Kerrisk, "Current Distribution and Inductance Calculations for Rail Gun Conductors," Los Alamos Scientific Laboratory Report LA-9092-MS, November 1981.
7. A. Wu, private communication.
8. G. C. Long, "Fundamental Limits to the Velocity of Solid Armatures in Railguns," PhD Dissertation, The University of Texas at Austin, June 1987.